INFLUENCE OF WELDING PROCESS ON FATIGUE CRACK PROPAGATION PROPERTIES IN STRUCTURAL STEEL

Geraldo de Paula Martins, gpm@cdtn.br
Emerson Giovani Rabello, egr@cdtn.br
Jefferson José Vilela, jjv@cdtn.br
Daniel Januário Cordeiro Gomes, danieljanuário@yahoo.com.br
Mariana Pimenta Alves, maripimenta8@yahoo.com.br
Comissão Nacional de Energia Nuclear/Centro de Desenvolvimento da Tecnologia Nuclear (CNEN/CDTN)

Leonardo Barbosa Godefroid, leonardo@em.demet.ufop.br
Universidade Federal de Ouro Preto (UFOP)

Carlos Alberto Cimini Jr, carlos.cimini@gmail.com
Universidade Estadual de Campinas (UNICAMPI)

Abstract. *On this work, the crack propagation resistance of the SAC 50 steel welded joints by the shielded metal arc weld (SMAW), gas tungsten arc weld (GTAW) and gas metal arc welding (GMAW) were studied. The crack propagation tests were accomplished using compact tension (CT) specimens with notch localized at the base metal (BM), heat affected zone (HAZ) and at the melting zone (MZ). Equations for Colliepriest, Priddle and Paris models for the several specimens tested were obtained and comparisons of the crack propagation properties for the three welding processes were made using the three models of crack propagation: Paris, Colliepriest and Priddle. It was concluded that the specimens with notch localized at the HAZ and at the MZ of the welding joints by the SMAW resulted in better crack propagation results. It was also concluded that for all situations, the Colliepriest model were the more near of the test data results.*

Keywords*: Fracture mechanics, Fatigue crack propagation, Fracture in welds, Fatigue crack propagation models.*

1. INTRODUCTION

The SAC50 steel is resistant at the atmospheric corrosion, and indicated for buildings, metallic bridges, and structures in general. This steel has the properties of the formation of a protective layer and is not necessary of paints. This imply in economy. Due to the several applications the component or structure manufactured with this steel that will be submitted to cyclic loads and any flaw existent into the material as a crack can to propagate from an initial crack to a critical crack and as a consequence to fracture. From these reason there are necessity to study the crack propagation resistance properties from crack propagation tests. The useful life can be determined using crack propagation models as the Paris-Erdogan model (Paris & Erdogan, 1960), the Colliepriest model (Barroso, 2004) and the Priddle model (Priddle, 1976). The Paris model, Equation 1, apply only at the region II (linear region) of the da/dN x ΔK curve in logarithm scale. The Colliepriest and Priddle models, Equations 2 and 3, apply to the three regions of the curve. These models can be compared with the data obtained from the tests and to check which them is the best representative of the real data.

$$\frac{da}{dN} = Cx\Delta K^n \tag{1}$$

$$Log\left(\frac{da}{dN}\right) = C_1 + C_2 xarctgh\left\{\frac{Log\left[\frac{\Delta K^2}{K_{Limiar}K_C(1-R^2)}\right]}{Log\left(\frac{K_C}{K_{Limiar}}\right)}\right\} \tag{2}$$

$$\frac{da}{dN} = Cx\left(\frac{\Delta K - \Delta K_{Limiar}}{K_C - K_{Máx}}\right) \tag{3}$$

2. MATERIALS AND METHODOLOGY

The material used in this work was the plate of SAC 50 steel with 12 mm of thickness. The welding process used was Shielded Metal Arc Welding (SMAW), Gas Metal Arc Welding (GMAW) and Gas Tungsten Arc Welding (GTAW), with the parameters of the Table 1.

Table 1. Parameters used in the welding process

Welding process	**SMAW**		**GTAW**		**GMAW**	
Voltage (V)	1/2V	V	1/2V	V	1/2V	V
Current (A)*	20	20	18 a 20	18 a 20	18 a 22	18 a 22
Welding rate (mm/min)	300	300	80	80	170	170
Filler metal	AWS E 7018G	AWS E 7018G	AWS ER 70S-6	AWS ER 70S-6	AWS ER 70S-6	AWS ER 70S-6
Shielding gas	-	-	Argon	Argon	C-25	C-25
Gas flow (l/min)	-	-	12	12	20	20

The first value corresponds to the first pass and the second value corresponds to the all passes.

From the welded joints were machined specimens for metallographic examination, tensile tests and fatigue crack propagation tests. The CT specimens for crack propagation tests were machined according ASTM E 647, with notch localized on the base metal (MB), melting zone (MZ) and heat affected zone (HAZ). The aim of the metallographic examination was to determine the microstructure of each region (BM, MZ and HAZ). The tensile tests were removed according the longitudinal and transversal orientations to the bead weld, for to obtain the yield stress at 0,2%, the curve stress and strain. The tension specimens were manufactured according the ASTM E 8M (2009). The crack propagation tests specimens were manufactured according ASTM E 647 (ASTM 647, 2008). Metallographic analysis of the BM, HAZ and MZ for the two processes from specimens obtained of longitudinal and transversal orientations to the weld bead were done. The specimens for crack propagation were pre-cracked by fatigue in 3 mm length, according ASTM E 647.

After the crack propagation tests, the Paris, Colliepriest and Priddle models were applied to the obtained data and numeric integration were made to obtain the number of cycles, for some specimens to compare with the obtained on the tests for at one of the welding process.

3. RESULTS AND DISCUSSION

Follow the results of tension, metallographic and fatigue crack propagation tests, with analysis through Colliepriest, Priddle and Paris models of the several data obtained from fatigue crack propagation tests.

3.1 Tension test results

On Tables 2, 3 and 4 are presented the results of tension tests obtained of the specimens removed from welded joints respectively SMAW GTAW e GMAW process.

Table 2. Results of longitudinal and transversal tension tests of the specimens removed from welded joints, 12mm in thickness, V bevel for SMAW process (ASTM E 8M, 2009)

	Specimen nº	σ_e at 0,2% [MPa]	σ_r [MPa]	$\Delta l/l$ [%]	Reduction of area (%)
Longitudinal	1	519	675	25,7	41,6
	2	539	676	25,7	41,6
	3	554	693	22,8	35,0
	Mean ± SD	537 ± 14	681 ± 8		
Transversal	4	480	603	17,0	31,7
	5	490	598	20,0	30,0
	6	470	592	20,0	31,7
	Mean ± SD	480 ± 8	597 ± 8		

Table 3. Results of longitudinal and transversal tension tests of the specimens removed from welded joints, 12mm in thickness, 1/2V bevel for GTAW process (ASTM E 8M, 2009)

	Specimen n°	σ_e at 0,2% [MPa]	σ_r [MPa]	Δl/l [%]	Reduction of area (%)
GTAW-transversal	1	449	580	11	38
	2	456	594	17	51
	3	452	583	17	52
	Mean ± SD	453 ± 3	586, ± 7	15	47
GTAW-longitudinal	7	484	619	22	71
	8	539	627	17	61
	9	561	657	17	72
	Mean ± SD	528 ± 39	634 ± 20	19	68

Table 4. Results of longitudinal and transversal tension tests of the specimens removed from welded joints, 12mm in thickness, 1/2V bevel for GMAW process (ASTM E 8M, 2000)

	Specimen n°	σ_e at 0,2% [MPa]	σ_r [MPa]	Δl/l [%]	Reduction of area (%)
GMAW-transversal	1	449	580	11	38
	2	456	594	17	51
	3	452	583	17	52
	Mean ± SD	453 ± 3	586 ± 7	15	47
GMAW-longitudinal	10	474	546	20	62
	11	481	548	16	59
	12	469	537	15	59
	Mean ± SD	475 ± 6	544 ± 6	17	60

3.2 Metallographic test results

On Figures 1 to 5 are presented micrographics of the several regions obtained of the welded joints.

The specimens of the BM analyzed presented a microstructure composed mainly of ferrite and pearlite (Figures 1a, 2a e 3a). Alcântara (2003) had determined the volumetric fraction of pearlite and ferrite and had obtained the ferrite grain size. The volumetric fraction of pearlite and ferrite were 18.63% and 81.37%, respectively with 1.21 in standard deviation. The grain size obtained were 7 µm, with standard deviation of 0.5. It can be to note the difference in microstructure of the BM for HAZ and MZ regions.

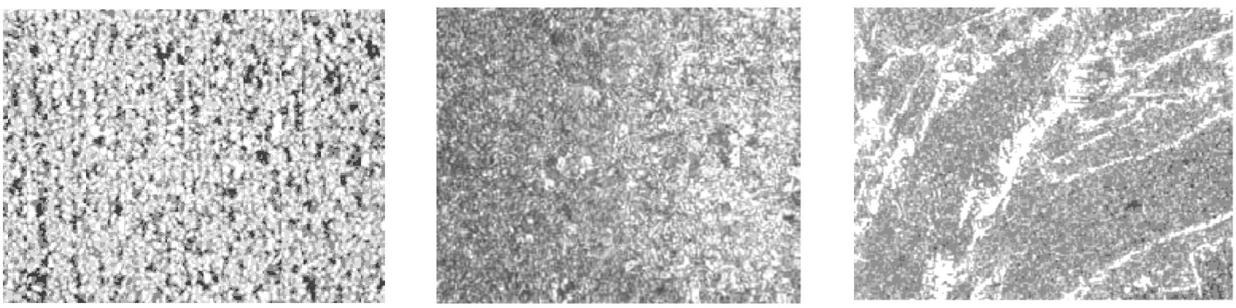

(a) (b) (c)

Figure 1. (a) BM, (b) HAZ and (c) MZ GTAW process

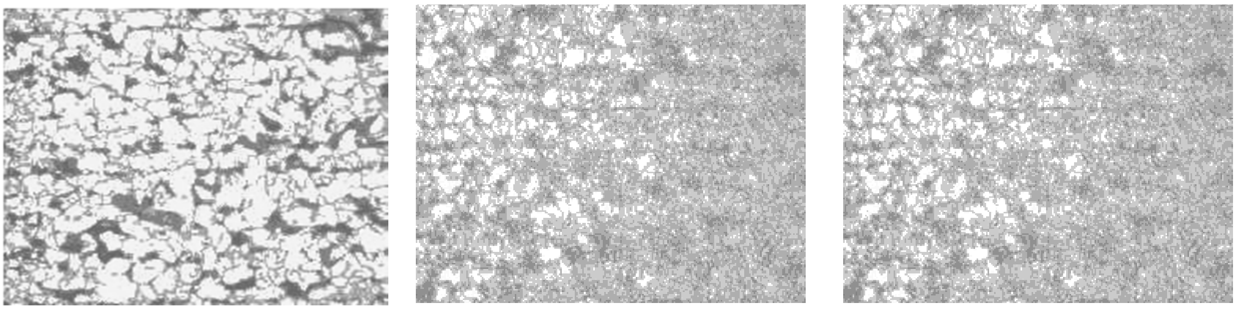

(a) (b) (c)

Figure 2. (a) BM, (b) HAZ and (c) MZ GMAW Process

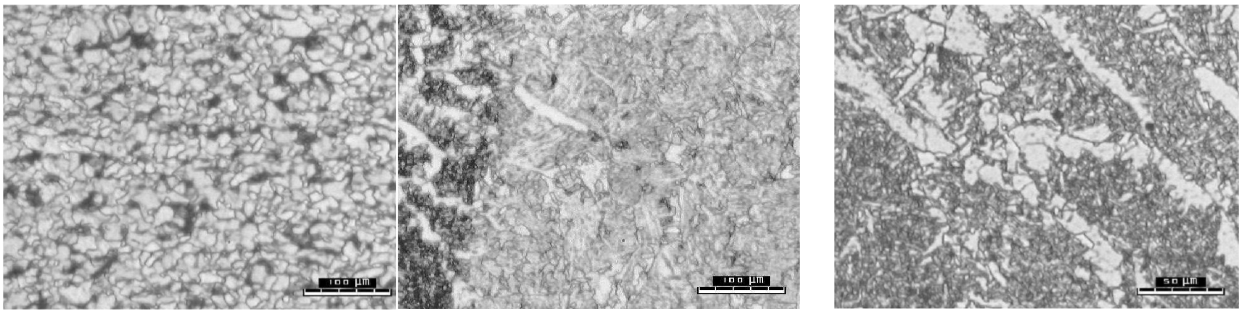

(a) (b) (c)

Figure 3. (a) BM, (b) HAZ and (c) MZ SMAW process

3.3 Fatigue crack results

Below (Figure from 4 to 6) are presented the crack propagation tests results for the several specimens.

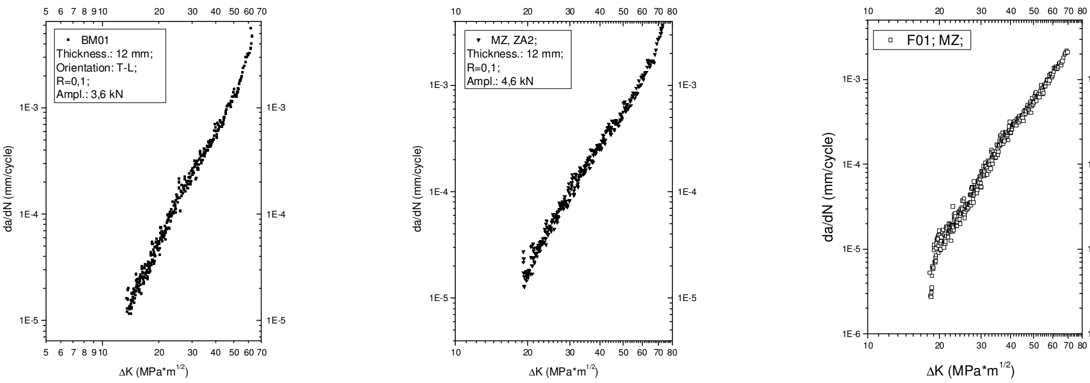

(a) (b) (c)

Figure 4. Graphic of fatigue crack propagation tests for SMAW specimens: (a) notch localized in BM region; (b) notch localized in HAZ region and (c) notch localized in MZ region.

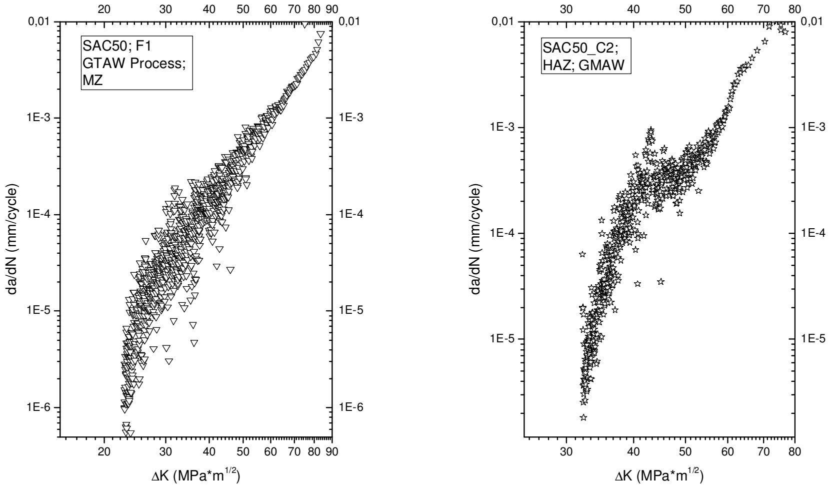

(a) (b)

Figure 5. Graphic of fatigue crack propagation tests for GTAW specimens: (a) notch localized in HAZ region and (b) notch localized in MZ region.

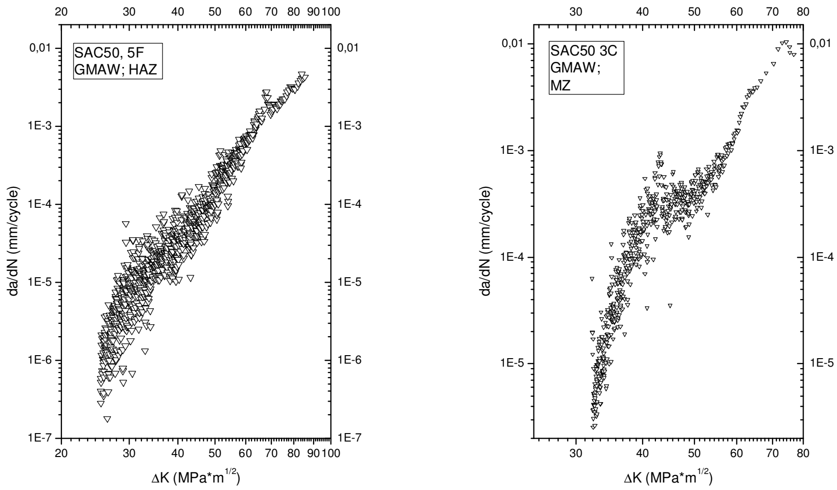

(a) (b)

Figure 6. Graphic of fatigue crack propagation tests for GMAW specimens: (a): notch localized in HAZ region and (b) notch localized in MZ region.

The ΔK_{Limiar} values were obtained by extrapolation of the da/dN values. They were bellow of 10^{-6} mm/cycle. These values were verified on the Colliepriest and Priddle models with a good approximation with the number of cycles obtained in the tests.

From the graphics of the figures 4, 5 and 6, it can be observed homogeneity for SMAW process, relatively to GTAW and GMAW processes with notch localized at MZ and HAZ regions. The results for specimens corresponding at GTAW process are better than the results of the specimens corresponding to GMAW process. It can be observed also a retard on the crack propagation rate for the specimens with notch localized on the MZ. This is probably due to compression at the Center of weld (Lal, 1994)

Bellow (Figure from 7 to 8 and Table from 5 to 8) are presented the graphics with application of the Colliepriest, Priddle and Paris models., for the specimens with notch on the MZ and HAZ for each one of the welding process.

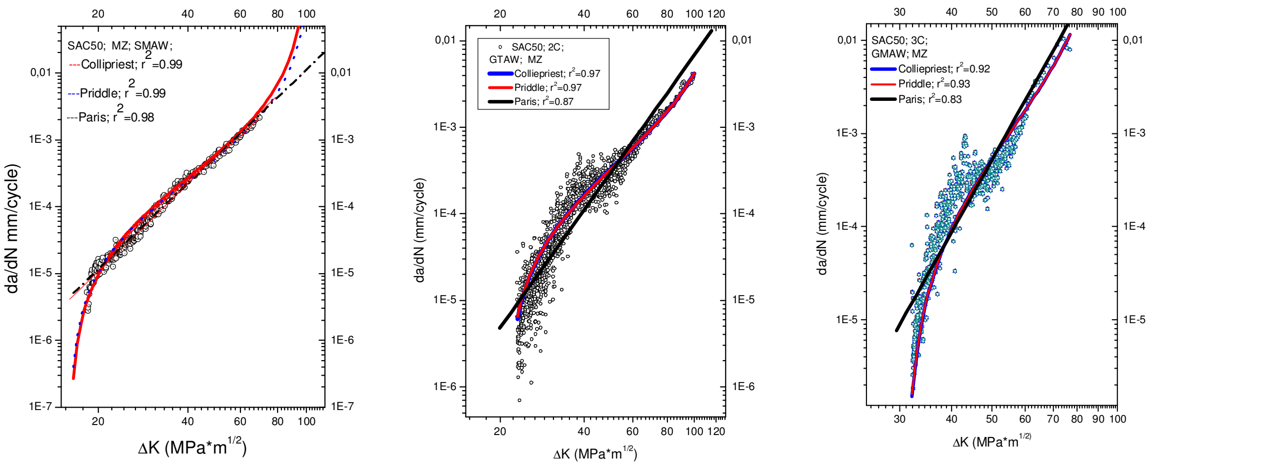

(a) (b) (c)

Figure 7. Colliepriest, Priddle and Paris models for the specimens with notch localized on the MZ: (a) SMAW, (b) GTAW and (c) GMAW; r^2= determination coefficient.

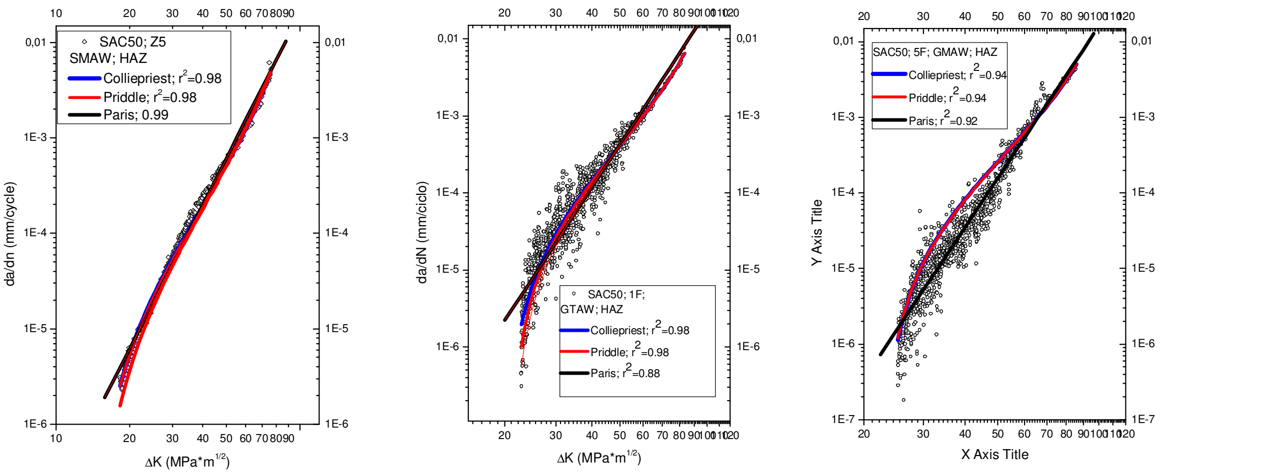

(a) (b) (c)

Figure 8. Colliepriest, Priddle and Paris models for the specimens with notch localized on the HAZ: (a) SMAW, (b) GTAW and (c) GMAW; r^2= determination coefficient

Table 5. Equations obtained for the models of the specimens with notch localized on the BM

Model	Paris	$\frac{da}{dN} = 1{,}22x10^{-9}\Delta K^{3{,}56}$
	Priddle	$\frac{da}{dN} = 9{,}7x10^{-4}\left(\frac{\Delta K - 10}{88 - 1{,}1x\Delta K}\right)^{1{,}52}$
	Colliepriest	$Log\left(\frac{da}{dN}\right) = -3{,}75 + 0{,}35xln\left[\frac{Log\left(\frac{\Delta K}{10}\right)^2}{Log\left(\frac{80}{\Delta K}\right)^2}\right]$

Table 6. Equations obtained of the several models for the SMAW process welded joints specimens

		Notch Localization	
		MZ	HAZ
Model	Paris		$\frac{da}{dN} = 4{,}61x10^{-12}\Delta K^{4{,}77}$
	Priddle	$\frac{da}{dN} = 2{,}23x10^{-3}\left(\frac{\Delta K - 15}{135 - 1{,}1x\Delta K}\right)^{1{,}77}$	$\frac{da}{dN} = 2{,}09x10^{-3}\left(\frac{\Delta K - 14}{125 - \Delta K}\right)^{2{,}10}$
	Colliepriest	$Log\left(\frac{da}{dN}\right) = -3{,}52 + 0{,}42xln\left[\frac{Log\left(\frac{\Delta K}{15}\right)^2}{Log\left(\frac{120}{\Delta K}\right)^2}\right]$	$Log\left(\frac{da}{dN}\right) = -3{,}47 + 0{,}49xln\left[\frac{Log\left(\frac{\Delta K}{14}\right)^2}{Log\left(\frac{114}{\Delta K}\right)^2}\right]$

Table 7. Equations obtained of the several models for the GTAW process welded joints specimens

		Notch Localization	
		MZ	HAZ
Model	Paris	$\frac{da}{dN} = 4{,}92x10^{-11}(\Delta K)^{3{,}99}$	$\frac{da}{dN} = 6{,}66x10^{-14}(\Delta K)^{5{,}77}$
	Priddle	$\frac{da}{dN} = 1{,}35x10^{-3}\left(\frac{\Delta K - 24}{148 - 1{,}1x\Delta K}\right)^{1{,}40}$	$\frac{da}{dN} = 2{,}75x10^{-3}\left(\frac{\Delta K - 21}{135 - 1{,}1x\Delta K}\right)^{1{,}93}$
	Colliepriest	$Log\left(\frac{da}{dN}\right) = -3{,}43 + 0{,}45xln\left[\frac{Log\left(\frac{\Delta K}{21}\right)^2}{Log\left(\frac{135}{\Delta K}\right)^2}\right]$	$Log\left(\frac{da}{dN}\right) = -3{,}43 + 0{,}32xln\left[\frac{Log\left(\frac{\Delta K}{21}\right)^2}{Log\left(\frac{120}{\Delta K}\right)^2}\right]$

Table 8. Equations obtained of the several models for the GMAW process welded joints specimens

		Notch Localization	
		MZ	HAZ
Model	Paris	$\frac{da}{dN} = 1{,}11x10^{-15}(\Delta K)^{6{,}87}$	$\frac{da}{dN} = 7{,}38x10^{-15}(\Delta K)^{6{,}08}$
	Priddle	$\frac{da}{dN} = 2{,}13x10^{-2}\left(\frac{\Delta K - 27}{148 - 1{,}1x\Delta K}\right)^{2{,}78}$	$\frac{da}{dN} = 1{,}71x10^{-3}\left(\frac{\Delta K - 23}{132 - 1{,}1x\Delta K}\right)^{2{,}10}$
	Colliepriest	$Log\left(\frac{da}{dN}\right) = -3{,}42 + 0{,}45xln\left[\frac{Log\left(\frac{\Delta K}{15}\right)^2}{Log\left(\frac{120}{\Delta K}\right)^2}\right]$	$Log\left(\frac{da}{dN}\right) = -3{,}36 + 0{,}50xln\left[\frac{Log\left(\frac{\Delta K}{23}\right)^2}{Log\left(\frac{120}{\Delta K}\right)^2}\right]$

On the Table 9 are presented the values in number of cycles obtained for the several specimens and the values calculated by Paris, Colliepriest and Priddle models for comparison.

Table 9. Comparison of Colliepriest, Priddle and Paris models with the obtained results in the tests

Welding process	Localization of the notch	Model			Test
		Colliepriest	Priddle	Paris	
	BM	521.901	504.588	128.095	528.300
SMAW	MZ	823.754	822.308	135.689	827.000
	HAZ	1.397.299	1.266.957	261.697	1.409.000
GTAW	MZ	908.304	856.213	60.285	910.000
	HAZ	1.513.797	1.504.848	863.651	1.529.000
GMAW	MZ	302.475	298.752	26.060	310.800
	HAZ	3.012.723	2.981.738	245.899	3.060.000

On Table 9 it is evident that the Colliepriest model is the most representative of the real data, followed by the Priddle model. The Paris model is very conservative because it is obtained through the data situated at the Region II of the sigmoidal curve l, Log(da/dN)xLog(ΔK) that, when applied at all data, Region I with very small rate propagation contribute for useful life.

5. CONCLUSIONS

1. The Colliepriest and Priddle models valid for the three regions of da/dN versus ΔK curve represent well the behavior of fatigue crack propagation. The Priddle model is more conservative than Colliepriest model;
2. Paris model is very conservative considering that it applies only at linear region of the curve (region II);
3. The inserted values from the obtained curve in a test with ΔK_{limiar} can be confirmed using the Colliepriest and Priddle models, comparing the obtained cycle numbers on the tests.

6. ACKNOWLEDGEMENTS

The authors thank Fundação de Amparo à Pesquisa do Estado de Minas Gerais (FAPEMIG), Conselho Nacional de Desenvolvimento Científico e Tecnológico (CNPq), Centro de Desenvolvimento da Tecnologia Nuclear (CDTN/CNEN) for supporting this work and technicians Geraldo A. S. Martins, Antônio Rocha and Emil Reis.

7. REFERENCES

American Society for Testing and Materials ASTM 647, 2008, Standard Method for Measurement of Fatigue Crack Growth Rates, Philadelphia, USA;

American Society for Testing and Materials, ASTM E 8M, 2009, Standard Test Methods for Tension Testing of Metallic Materials. Philadelphia, 2000;

Barroso, E. K. L., 2004, "Efeito da Pré-Deformação e Shot Peening na Tenacidade à Fratura e Propagação de Trinca por Fadiga da Liga de Alumínio 7475-T7351, da Aplicação Aeronáutica", Dissertação de Mestrado, Universidade Federal de Ouro Preto, Programa de Pós Graduação em Engenharia de Materiais, Ouro Preto, MG, Brasil;

LAL, D.N., 1994, "A New Mechanistic Approach to Analyzing LEFM Fatigue Crack Growth Behavior of Metals and Alloys". Engineering Fracture Mechanics, vol. 47, nº 3, pp. 379-401.

Paris, P. C. and Erdogan, F., "A Critical Analysis of Crack Propagation Laws." Journal of Basic Engineering, Vol. 85, pp. 528-534, 1960;

Priddle, E. K., 1976. "High Cycle Fatigue Crack Propagation under Random and Constant Amplitude Loadings." International Journal of Pressure Vessels and Piping, 4, pp. 89-117;

5. RESPONSIBILITY NOTICE